



RESEARCH ARTICLE | JULY 21 2020

A practical model of twin-beam experiments for sub-shot-noise absorption measurements

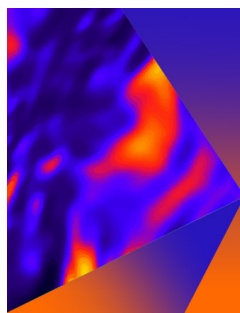
Special Collection: [Quantum Sensing with Correlated Light Sources](#)

Jason D. Mueller ; Nigam Samantaray; Jonathan C. F. Matthews 



Appl. Phys. Lett. 117, 034001 (2020)

<https://doi.org/10.1063/5.0015576>



Applied Physics Letters

Special Topic: Mid and Long Wavelength Infrared Photonics, Materials, and Devices

Submit Today



A practical model of twin-beam experiments for sub-shot-noise absorption measurements

Cite as: Appl. Phys. Lett. **117**, 034001 (2020); doi: [10.1063/5.0015576](https://doi.org/10.1063/5.0015576)

Submitted: 29 May 2020 · Accepted: 8 July 2020 ·

Published Online: 21 July 2020



View Online



Export Citation



CrossMark

Jason D. Mueller,^{a)} Nigam Samantaray, and Jonathan C. F. Matthews^{b)}

AFFILIATIONS

Quantum Engineering Technology Labs, H. H. Wills Physics Laboratory and Department of Electrical and Electronic Engineering, University of Bristol, Bristol BS8 1FD, United Kingdom

Note: This paper is part of the APL Special Collection on Quantum Sensing with Correlated Light Sources.

^{a)}Author to whom correspondence should be addressed: jason.mueller93@yahoo.com

^{b)}Electronic mail: jonathan.matthews@bristol.ac.uk

ABSTRACT

Quantum-intensity-correlated twin beams of light can be used to measure absorption with precision beyond the classical shot-noise limit. The degree to which this can be achieved with a given estimator is defined by the quality of the twin-beam intensity correlations, which is quantified by the noise reduction factor. We derive an analytical model of twin-beam experiments, incorporating experimental parameters such as the relative detection efficiency of the beams, uncorrelated optical noise, and uncorrelated detector noise. We show that for twin beams without excessive noise, measured correlations can be improved by increasing the detection efficiency of each beam; notwithstanding, this may unbalance detection efficiency. However, for beams with excess intensity or other experimental noise, one should balance detection efficiency, even at the cost of reducing detection efficiency—we specifically define these noise conditions and verify our results with statistical simulation. This has application in design and optimization of absorption spectroscopy and imaging experiments.

Published under license by AIP Publishing. <https://doi.org/10.1063/5.0015576>

Optical shot-noise is present in all classical imaging and spectroscopy applications using light and can limit the measurement precision of a parameter once all other technical noise sources have been accounted for.^{1–6} Using quantum-intensity-correlated light beams (i.e., twin beams)^{7–11} is one method to surpass this classical limit and obtain greater absorption-measurement precision for a given optical power.¹² Experiments demonstrating this concept have been performed at near-infrared wavelengths using approximately wavelength-degenerate twin beams from downconversion.^{9–11,13–15} Monochromatically pumped Four-Wave Mixing (FWM) generates energy-conserving twin beams that are of non-degenerate wavelengths that straddle the pump wavelength. This is useful for imaging and spectroscopy applications because FWM can be implemented with a range of materials and pump wavelengths, providing access to a range of twin-beam wavelengths above and below the near-infrared.^{16–21} However, the measurement of highly non-degenerate correlated beams can result in unbalanced detection efficiency, with uncorrelated optical and detector noise present regardless of wavelength degeneracy.

Previous work on measuring quantum intensity correlations from wavelength-degenerate spontaneous downconversion sources has approximated that (1) because the wavelengths are degenerate, so

are the loss and detection efficiency of both beams and (2) there is negligible excess optical or detector noise.^{9,10,14,22,23} Under these assumptions, measured intensity correlations scale with channel efficiency as $1 - \eta$ and can always be improved by reducing loss or improving detector efficiency. Here, we show that if either assumption is not true, the scaling of measured intensity correlations depends on the relative twin-beam detection efficiency and properties of the excess noise, and correlations may be improved by reducing the efficiency of one detection channel or unbalancing detection.

In this paper, we present a general analytical framework for twin-beam experiments characterized by intensity-difference measurements, extending previous work based on detector calibration²⁴ and high-power twin beams.²⁵ Our model outputs the Noise-Reduction Factor (NRF), a quantifier of twin-beam correlations,^{9–11,24–26} with unbalanced detection loss, uncorrelated optical noise, and uncorrelated detector noise as variables. It is agnostic to the sources of the uncorrelated noise and only requires basic experimental characterization of their mean intensity and variance. We evidence that to improve the quality of measured twin-beam correlations, one should either maximize detection efficiency of both beams or balance detection efficiency, depending on the properties of the experimental noise. We then

confirm our model with statistical simulations and give a specific real-world example modeling a FWM experiment.

The Fano factor^{27,28} quantifies the intensity noise of a single optical beam, labeled i , according to

$$F_i = \frac{\text{Var}[N_i]}{E[N_i]}, \quad (1)$$

where N_i is the random variable associated with the beam's photon number (i.e., intensity), characterized by variance $\text{Var}[N_i]$ and mean value $E[N_i]$. Classically accessible super-Poissonian intensity fluctuations correspond to $F_i > 1$, while Poisson-distributed statistics, which can be achieved by measuring the intensity of a coherent state, correspond to the classical limit of $F_i = 1$. Individual beams exhibiting $0 \leq F_i < 1$ are uniquely non-classical and classified as sub-Poissonian.

The Fano factor can be an important quantifier when searching for optical beams for parameter estimation, as the intensity noise of a probe beam maps onto the uncertainty of estimating a physical parameter, such as absorption.¹³ A beam with $F < 1$ is a resource for measuring absorption with precision beyond the classical limit. It is also possible to use a beam with $F \geq 1$ for measuring parameters with precision beyond the classical limit, provided that the beam is sufficiently well-correlated with another beam that can be measured.^{9,10}

To quantify the mutual noise characteristics of two beams, we use the NRF, given as^{9–11,24–26}

$$\sigma = \frac{\text{Var}[N_1 - N_2]}{E[N_1 + N_2]}. \quad (2)$$

Note that some authors use a modified form of the NRF, where $N_2 \rightarrow (E[N_1]/E[N_2])N_2$ to account for the detection-efficiency mismatch.^{11,25} Our analysis assumes the form in Eq. (2) and may be straightforwardly modified to accommodate this alternate NRF definition.

Values of $\sigma \geq 1$ correspond to separable classical beams, with $\sigma = 1$ representing the classical limit of two Poisson-distributed beams. Values of $0 \leq \sigma < 1$ correspond to non-classical twin-beam intensity correlations. However, this alone is insufficient to achieve parameter estimation with precision better than what can be achieved with a single pass of a single beam with $F = 1$, defined as the classical Shot-Noise Limit (SNL).^{9–11} Sub-SNL parameter estimation is also linked to the choice of estimator (see [supplementary material Appendix A](#)).

We describe two correlated twin beams $i = 1, 2$ with intensity mean and variance

$$E[N_i] = \eta_i E[N], \quad (3)$$

$$\text{Var}[N_i] = E[N_i] + \beta E[N_i]^2, \quad (4)$$

where N is the lossless photon number, equal among both beams due to the energy-conserving nature of twin-beam production. The parameter $0 \leq \eta_i \leq 1$ is the total efficiency of each beam's optical path (i.e., channel efficiency), comprising loss from all optical components and detection efficiency. The parameter $\beta \geq 0$ is used to account for super-Poissonian intensity fluctuations of the individual beams of the twin-beam system,^{29–32} and is equivalent to the second-order intensity correlation function $g^{(2)}(0) - 1$.³²

We may write the lossy twin-beam variance in terms of the lossless photon number, Fano factor F , using $\beta E[N] = F - 1$,

$$\text{Var}[N_i] = \eta_i E[N] + \eta_i^2 (F - 1) E[N]. \quad (5)$$

Using Eqs. (5) and (3) in Eq. (2) yields

$$\sigma = 1 - \underbrace{\frac{2\eta_1\eta_2}{\eta_1 + \eta_2}}_{\sigma_p} + \underbrace{\frac{(\eta_1 - \eta_2)^2 (F - 1)}{\eta_1 + \eta_2}}_{\sigma_{sp}}, \quad (6)$$

where we use the covariance $\text{Cov}[N_1, N_2] = \eta_1\eta_2(E[N] + \beta E[N]^2)$.^{29–31,33} The first two terms of Eq. (6) (σ_p) correspond to correlated coherent-state intensity fluctuations. The final term (σ_{sp}) is the contribution to the NRF associated with super-Poissonian intensity fluctuations. Importantly, σ_{sp} has a dependence on the channel-efficiency mismatch and Fano factor; the minimum of σ is, therefore, found by differentiating Eq. (6) with respect to η_2 and considering the boundary conditions, namely, $0 \leq \eta_2 \leq 1$,

$$\eta_2 = \begin{cases} 1, & 1 \leq F \leq F' \\ \eta_1 \left(\sqrt{4 + \frac{2}{F-1}} - 1 \right), & F > F', \end{cases} \quad (7)$$

where $F' = (\eta_1^2 - 2\eta_1 - 1)/(3\eta_1^2 - 2\eta_1 - 1)$. This result is presented graphically in Fig. 1, where if F is smaller than the threshold F' , then increasing channel efficiency improves measured twin-beam correlations. For large F , it becomes crucial to balanced detection according to Eq. (7) ($\eta_2 \rightarrow \eta_1$) due to the quadratically increasing term in σ_{sp} .

We now demonstrate the detrimental effects of uncorrelated noise photons and uncorrelated detector noise on the measured NRF. Uncorrelated optical noise may come from resonant and non-resonant optical processes within the material used for twin-beam generation, such as fluorescence or broadband Raman scattering caused by the pump beam. Optical noise can also be associated with scattered or ambient light. Detector noise may be associated with photodiode dark current or CCD dark counts. The following derived model is general enough to account for all these sources of noise. For simplicity, we include optical noise N_p on only one detection channel as $N_2 \rightarrow N_2 + N_p$, and the procedure may be similarly adapted to accommodate

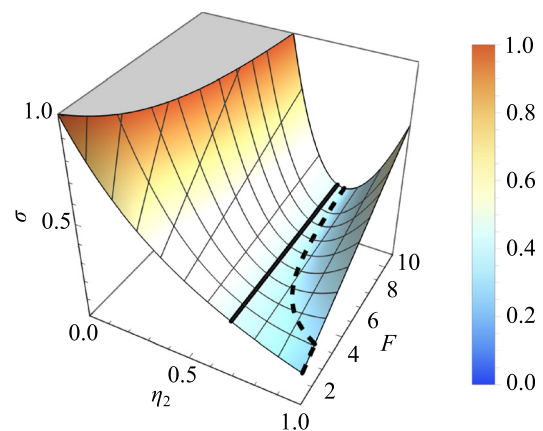


FIG. 1. The NRF from Eq. (6) scaling with relative channel efficiency (given $\eta_1 = 0.7$) is shown for values of F from 1 to 10. The minimum NRF is indicated by the dashed line, according to Eq. (7). The solid line indicates perfectly balanced detection, $\eta_2 = \eta_1$, to show the convergence of the minimum NRF for large F .

independent noise on N_1 as well (see [supplementary material Appendix B](#)).

We define the optical noise to have the following realistic properties: (1) the efficiency for detecting the correlated-signal and uncorrelated-noise photons on channel 2 is assumed to be the same: $\eta_o = \eta_2$; (2) the mean noise intensity is some fraction $\rho \geq 0$ of the mean signal intensity: $E[N_\rho] = \eta_2 \rho E[N]$; (3) the Fano factor of the optical noise F_ρ before channel loss can be written as $F_\rho - 1 = \rho(F - 1) \geq 0$, according to Eq. (4); and (4) the optical noise photons are generated via a process distinct from the signal photons: $\text{Cov}[N_1, N_\rho] = \text{Cov}[N_2, N_\rho] = 0$. Similar to Eq. (5), we have

$$\text{Var}[N_\rho] = \eta_2 \rho E[N] + \eta_2^2 \rho (F_\rho - 1) E[N]. \quad (8)$$

When considering detector noise, we assume it to be the same for both channels, $N_{\{1,2\}} \rightarrow N_{\{1,2\}} + N_d$ (see [supplementary material Appendix B](#) for unbalanced detector noise). Let the mean dark counts of each detector $E[N_d]$ be some fraction d of the optical signal $E[N]$, independent of η_1 and η_2 , with corresponding Fano factor F_d . Although detector noise cannot be explicitly derived from the optical signal, characterizing experimental parameters allows one to draw this equivalence. The variance of the detector noise may be written as

$$\text{Var}[N_d] = dE[N] + d(F_d - 1)E[N]. \quad (9)$$

We note the covariance for each detector with each other and the optical signal is zero because they are uncorrelated.

Finally, we can write the NRF for individually super-Poissonian twin beams, accounting for uncorrelated, super-Poissonian optical and detector noise, combining the results of Eqs. (8) and (9) in Eq. (2): $\sigma = \sigma_p + \sigma_{sp} + \sigma_\rho + \sigma_d$, with

$$\sigma_p = 1 - \frac{2\eta_1\eta_2}{\eta_1 + (1+\rho)\eta_2 + 2d}, \quad (10a)$$

$$\sigma_{sp} = \frac{(\eta_1 - \eta_2)^2(F - 1)}{\eta_1 + (1+\rho)\eta_2 + 2d}, \quad (10b)$$

$$\sigma_\rho = \frac{\eta_2^2 \rho (F_\rho - 1)}{\eta_1 + (1+\rho)\eta_2 + 2d}, \quad (10c)$$

$$\sigma_d = \frac{2d(F_d - 1)}{\eta_1 + (1+\rho)\eta_2 + 2d}, \quad (10d)$$

where σ_p and σ_d are the optical and detector noise contributions to the NRF, respectively.

Similar to before, we can now calculate the relative channel efficiency required to obtain the minimum NRF. Assuming that detector noise is much less than optical noise, $d \ll \rho$, as may be the case for bright optical signals or low-noise detection, this minimum is achieved when

$$\eta_2 = \begin{cases} 1, & 1 \leq F \leq F'' \\ \frac{\eta_1}{1+\rho} \left(\sqrt{2 + \frac{2(2\rho F + F - \rho)}{(F-1)(1+\rho^2)}} - 1 \right), & F > F'', \end{cases} \quad (11)$$

where $F'' = 1 - 2\eta_1^2/[\eta_1^2(\rho + 3) - (2\eta_1 + \rho + 1)(1 + \rho^2)]$. As optical noise increases in Eq. (11), $\eta_2 \rightarrow 0$ and $\sigma \rightarrow F$. This result highlights the importance of reducing optical noise on the twin beams to minimize the NRF.

For specific values characterizing the optical signal and optical and detector noise, we can compare, as in Fig. 2, the behavior of the NRF as relative channel efficiency is varied, from the ideal Poissonian twin-beam case to the full model including uncorrelated optical and detector noise [see Eqs. (10a)–(10d)]. In the ideal case, one always measures sub-Poissonian correlations when including a quantum-correlated twin beam. Using example values for the parameters of Eqs. (10a)–(10d) to illustrate how the model can be used to quantify the detrimental effects of noise, as shown in Fig. 2, the minimum-attainable NRF increases, and sub-Poissonian twin-beam correlations may not be measurable despite the underpinning quantum correlations between the beams.

We now derive an example scenario for a proposed twin beam experiment based on a stimulated FWM formalism to illustrate the effects of noise at various optical powers and how experimental parameters may be optimized. This example scenario shows similar features to high-gain downconversion experiments,^{8,25} and the model may also be applied in the spontaneous-emission regime.^{9,15,23} We make the following three assumptions: (1) twin-beam power increases exponentially with pump power p as $E[N] \propto pe^{\lambda p}$, for some constant $\lambda > 0$; (2) optical noise power increases linearly with pump power as $E[N_\rho] \propto p$; and (3) mean detector noise increases linearly with, e.g., the integration time or size, or temperature w , and has some constant readout noise, but is independent of p : $E[N_d] \propto w + \lambda$, for some other constant $\lambda > 0$.

Assumption (1) is true if, for example, twin beams are generated in-fiber via monochromatically pumped FWM in the exponential-gain regime, through parametric amplification.³⁴ Assumption (2) may represent optical noise sources such as Raman scattering at wavelengths far from the pump, where the phonon density of states is low.^{35,36} Assumption (3) represents thermal detector noise (linear

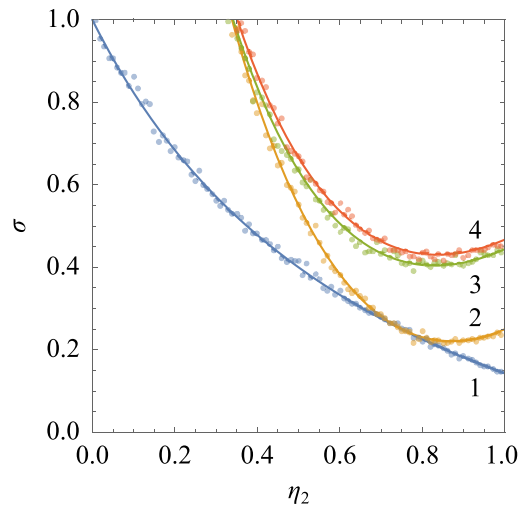


FIG. 2. The NRF scaling with relative channel efficiency ($\eta_1 = 0.75$) is shown for example experimental parameters. (1) Poissonian twin beams ($F = 1$); (2) super-Poissonian twin beams ($F = 4$); (3) super-Poissonian twin beams with uncorrelated super-Poissonian optical noise ($\rho = 0.45$ and $F_\rho = 1.2$); (4) super-Poissonian twin beams with uncorrelated super-Poissonian optical and detector noise ($d = 0.01$ and $F_d = 3$). Correspondingly colored points represent statistical simulation results, showing close agreement with theory (details in [supplementary material Appendix C](#)). Note that in plot 4, σ equals Fano and detector noise for $\eta_2 = 0$ [see Eqs. (10a)–(10d)] and is, therefore, greater than one.

contribution in w) and constant readout noise, typical for photodiode³⁷ and CCD³⁸ detectors. Thus, we may write the terms of Eqs. (10a)–(10d) as

$$F(p) = 1 + \lambda_1 p e^{\lambda_2 p}, \quad (12a)$$

$$F_p(p) = 1 + \lambda_3 p, \quad (12b)$$

$$F_d(w) = 1 + \lambda_4 + \lambda_5 w, \quad (12c)$$

$$\rho(p) = \lambda_6 e^{-\lambda_7 p}, \quad (12d)$$

$$d(p, w) = (\lambda_8 w + \lambda_9) p^{-1} e^{-\lambda_{10} p}, \quad (12e)$$

where $\Lambda = \{\lambda_1, \dots, \lambda_{10} > 0\}$ are fit parameters of the proposed experiment's model. Equations (12a)–(12e) are found by direct substitution of Assumptions (1)–(3) into Eq. (4), with $\beta > 0$, and Eqs. (12d) and (12e) by substitution into the definitions of ρ and d . Although detector noise is fundamentally independent of pump power, their relative intensities can still be compared using this substitution, as in Eq. (12e). The NRF is plotted in Fig. 3 as a function of pump power, using Eqs. (10a)–(10d) and (12a)–(12e), to show how various noise sources impact measured correlations.

In Fig. 3(a), detector noise is dominant at lower optical power, as the signal-to-noise ratio is low in this regime; indeed, as $p \rightarrow 0$, then $\sigma \rightarrow F_d$, as expected. Increasing uncorrelated optical noise in Fig. 3(b) has a more significant effect at low and intermediate pump powers, highlighting the importance of filtering optical noise.

As the signal-to-noise ratio increases in Fig. 3(c) at higher pump powers due to the different scalings of $E[N]$, $E[N_p]$, and $E[N_d]$, balancing channel efficiency becomes the critical task. This is because the Fano factor of our considered example scales exponentially in pump power, and so σ_{sp} diverges quickly when $\eta_1 \neq \eta_2$, as seen in Fig. 1. Indeed, $\eta_2 = 0.8$ outperforms $\eta_2 = 1$ in Fig. 3(c), despite being lower channel efficiency. High-power intensity-correlation experiments should, therefore, implement classical noise suppression to reduce F ,³⁹ or appropriately balance channel efficiency, to measure sub-Poissonian correlations.

We have derived a model of twin-beam intensity correlations, which accounts for experimental limitations such as uncorrelated optical and detector noise and unbalanced detection efficiency. From this model, we analytically and numerically show that for beams with excess noise below a well-defined threshold, measured correlations can be improved by maximizing the detection efficiency of both beams. However, for beams with intensity or experimental noise beyond this threshold, one should appropriately balance detection efficiency, even at the cost of reducing channel efficiency. The parameters required to determine this threshold and to maximize the quality of measured twin-beam correlations are experimentally accessible,^{8,9,11,25} and can be optimized by simulating the resulting behavior of different values using our model.

We have also demonstrated the utility of this model for an example FWM experimental scenario. While we have only considered this specific example, the model and the techniques used to derive it apply to many similar experiments, from wavelength-degenerate downconversion experiments dominated by detector noise to non-wavelength-degenerate FWM experiments dominated by optical noise.^{9,11–15,25,26}

Higher-power measurements find more applications than intensities associated with squeezed vacuum and photon counting experiments. We, therefore, believe that this model will find use as optical quantum metrology targets practical applications at microwatts to milliwatts of optical power and exotic wavelengths beyond the near-

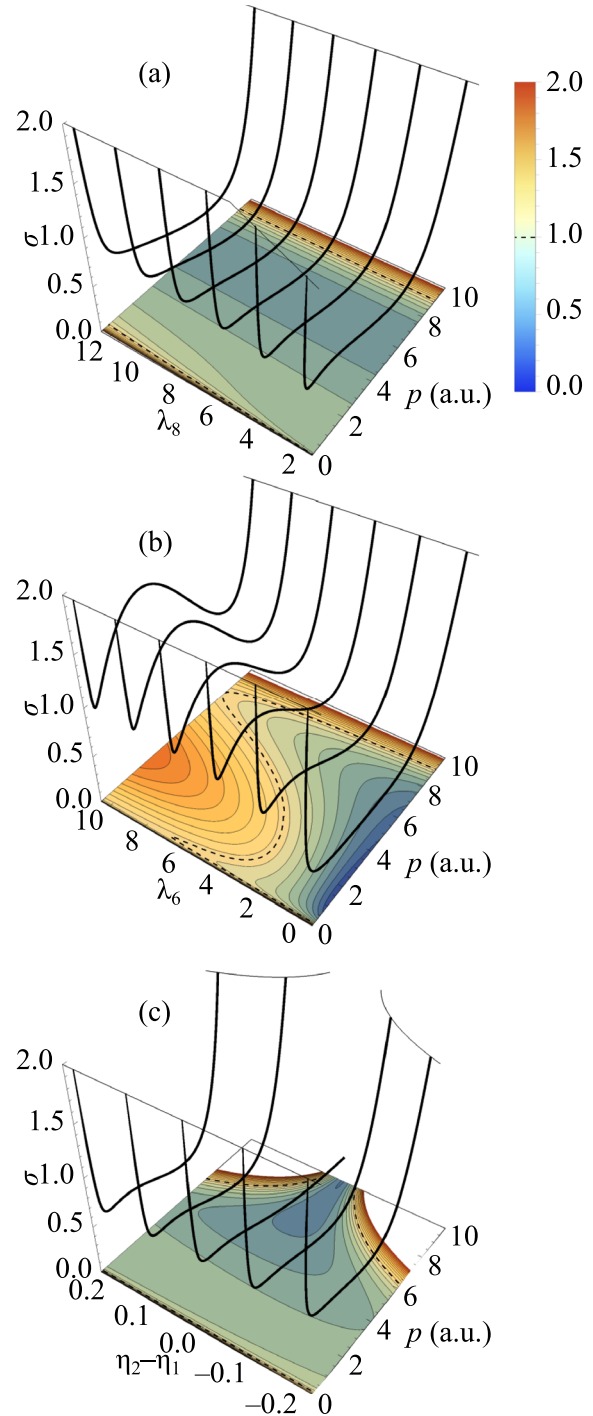


FIG. 3. The NRF plotted against pump power for varying experimental parameters, with contour plots projected beneath: (a) increasing detector noise parameter λ_8 , (b) increasing optical noise parameter λ_6 , and (c) varying relative channel efficiency $\eta_2 - \eta_1$ [see Eqs. (12a)–(12e)]. The default parameters for this simulation are $\Lambda = \{0.00\ 005, 0.01, 0.01, 0.5, 0.1, 1, 0.005, 1.001, 0, 0.005\}$, with $\eta_1 = 0.75$ and $\eta_2 = 0.7$, chosen to demonstrate the general features of the described FWM experiment. Dashed lines represent the $\sigma = 1$ contour, and the scale bar is fixed for all plots.

infrared, using high-gain twin-beam experiments to enhance measurement precision.

See the [supplementary material](#) for an analysis of twin-beam absorption estimators, a NRF model that considers independent optical and detector noise on both channels, and details of simulations related to [Fig. 2](#).

We thank E. Allen, M. Chekhova, and J. Rarity for helpful discussions. This work was supported by QuantIC—The UK Quantum Technology Hub in Quantum Imaging, EPSRC Grant No. EP/T00097X/1. J.D.M. was supported by the Quantum Engineering Centre for Doctoral Training, EPSRC Grant No. EP/L015730/1. J.C.F.M. acknowledges fellowship support from EPSRC Grant No. EP/M024385/1 and ERC starting Grant No. ERC-2018-STG803665.

DATA AVAILABILITY

The data that support the findings of this study are openly available in data.bris at <https://doi.org/10.5523/bris.axp4yp1om05m2-hapqz5cd5xyo>, [Ref. 40].

REFERENCES

- M. Celebrano, P. Kukura, A. Renn, and V. Sandoghdar, "Single-molecule imaging by optical absorption," *Nat. Photonics* **5**, 95–98 (2011).
- P. Kukura, M. Celebrano, A. Renn, and V. Sandoghdar, "Single-molecule sensitivity in optical absorption at room temperature," *J. Phys. Chem. Lett.* **1**, 3323–3327 (2010).
- M.-H. Chien, M. Bramehuber, B. K. Rossboth, G. J. Schütz, and S. Schmid, "Single-molecule optical absorption imaging by nanomechanical photothermal sensing," *Proc. Natl. Acad. Sci.* **115**, 11150–11155 (2018).
- J. Miyazaki, H. Tsurui, A. Hayashi-Takagi, H. Kasai, and T. Kobayashi, "Sub-diffraction resolution pump-probe microscopy with shot-noise limited sensitivity using laser diodes," *Opt. Express* **22**, 9024–9032 (2014).
- Y. Ozeki, Y. Kitagawa, K. Sumimura, N. Nishizawa, W. Umemura, S. Kajiyama, K. Fukui, and K. Itoh, "Stimulated Raman scattering microscope with shot noise limited sensitivity using subharmonically synchronized laser pulses," *Opt. Express* **18**, 13708–13719 (2010).
- E. Betzig, A. Lewis, A. Harootunian, M. Isaacson, and E. Kratschmer, "Near field scanning optical microscopy (NSOM): Development and biophysical applications," *Biophys. J.* **49**, 269–279 (1986).
- S. Reynaud, C. Fabre, and E. Giacobino, "Quantum fluctuations in a two-mode parametric oscillator," *J. Opt. Soc. Am. B* **4**, 1520–1524 (1987).
- A. Heidmann, R. J. Horowicz, S. Reynaud, E. Giacobino, C. Fabre, and G. Camy, "Observation of quantum noise reduction on twin laser beams," *Phys. Rev. Lett.* **59**, 2555–2557 (1987).
- P.-A. Moreau, J. Sabines-Chesterking, R. Whittaker, S. K. Joshi, P. M. Birchall, A. McMillan, J. G. Rarity, and J. C. F. Matthews, "Demonstrating an absolute quantum advantage in direct absorption measurement," *Sci. Rep.* **7**, 1–7 (2017).
- G. Brida, M. Genovese, and I. R. Berchera, "Experimental realization of sub-shot-noise quantum imaging," *Nat. Photonics* **4**, 227 (2010).
- E. Losero, I. Ruo-Berchera, A. Meda, A. Avella, and M. Genovese, "Unbiased estimation of an optical loss at the ultimate quantum limit with twin-beams," *Sci. Rep.* **8**, 1–11 (2018).
- E. Jakeman and J. Rarity, "The use of pair production processes to reduce quantum noise in transmission measurements," *Opt. Commun.* **59**, 219–223 (1986).
- R. Whittaker, C. Erven, A. Neville, M. Berry, J. L. O'Brien, H. Cable, and J. C. F. Matthews, "Absorption spectroscopy at the ultimate quantum limit from single-photon states," *New J. Phys.* **19**, 023013 (2017).
- N. Samantaray, I. Ruo-Berchera, A. Meda, and M. Genovese, "Realization of the first sub-shot-noise wide field microscope," *Light* **6**, e17005 (2017).
- J. Sabines-Chesterking, R. Whittaker, S. K. Joshi, P. M. Birchall, P. A. Moreau, A. McMillan, H. V. Cable, J. L. O'Brien, J. G. Rarity, and J. C. F. Matthews, "Sub-shot-noise transmission measurement enabled by active feed-forward of heralded single photons," *Phys. Rev. Appl.* **8**, 014016 (2017).
- Y. Chen, W. Wadsworth, and T. Birks, "Ultraviolet four-wave mixing in the LP₀₂ fiber mode," *Opt. Lett.* **38**, 3747–3750 (2013).
- B. Sévigny, A. Cassez, O. Vanvincq, Y. Quiquempois, and G. Bouwmans, "High-quality ultraviolet beam generation in multimode photonic crystal fiber through nondegenerate four-wave mixing at 532 nm," *Opt. Lett.* **40**, 2389–2392 (2015).
- H. Pourbeyram, E. Nazemosadat, and A. Mafi, "Detailed investigation of intermodal four-wave mixing in SMF-28: Blue-red generation from green," *Opt. Express* **23**, 14487–14500 (2015).
- H. Pourbeyram and A. Mafi, "Photon pair generation in multimode optical fibers via intermodal phase matching," *Phys. Rev. A* **94**, 023815 (2016).
- A. S. Kowligy, D. D. Hickstein, A. Lind, D. R. Carlson, H. Timmers, N. Nader, D. L. Maser, D. Westly, K. Srinivasan, S. B. Papp, and S. A. Diddams, "Tunable mid-infrared generation via wide-band four-wave mixing in silicon nitride waveguides," *Opt. Lett.* **43**, 4220–4223 (2018).
- Y. Sebbag, Y. Barash, and U. Levy, "Generation of coherent mid-IR light by parametric four-wave mixing in alkali vapor," *Opt. Lett.* **44**, 971–974 (2019).
- M. Vasilyev, S.-K. Choi, P. Kumar, and G. M. D'Ariano, "Tomographic measurement of joint photon statistics of the twin-beam quantum state," *Phys. Rev. Lett.* **84**, 2354–2357 (2000).
- M. Bondani, A. Allevi, G. Zambra, M. G. A. Paris, and A. Andreoni, "Sub-shot-noise photon-number correlation in a mesoscopic twin beam of light," *Phys. Rev. A* **76**, 013833 (2007).
- G. Brida, I. P. Degiovanni, M. Genovese, M. L. Rastello, and I. Ruo-Berchera, "Detection of multimode spatial correlation in PDC and application to the absolute calibration of a CCD camera," *Opt. Express* **18**, 20572–20584 (2010).
- T. S. Iskhakov, V. C. Usenko, U. L. Andersen, R. Filip, M. V. Chekhova, and G. Leuchs, "Heralded source of bright multi-mode mesoscopic sub-poissonian light," *Opt. Lett.* **41**, 2149–2152 (2016).
- M. A. Finger, T. S. Iskhakov, N. Y. Joly, M. V. Chekhova, and P. S. J. Russell, "Raman-free, noble-gas-filled photonic-crystal fiber source for ultrafast, very bright twin-beam squeezed vacuum," *Phys. Rev. Lett.* **115**, 143602 (2015).
- U. Fano, "Ionization yield of radiations. II. The fluctuations of the number of ions," *Phys. Rev.* **72**, 26–29 (1947).
- H. A. Bachor and T. C. Ralph, *A Guide to Experiments in Quantum Optics* (John Wiley & Sons, Ltd., 2019), pp. 93–137.
- E. M. Purcell, "The question of correlation between photons in coherent light rays," *Nature* **178**, 1449–1450 (1956).
- L. Mandel, "Fluctuations of photon beams and their correlations," *Proc. Phys. Soc.* **72**, 1037–1048 (1958).
- L. Mandel, "Fluctuations of photon beams: The distribution of the photo-electrons," *Proc. Phys. Soc.* **74**, 233–243 (1959).
- L. Mandel, "Non-classical states of the electromagnetic field," *Phys. Scr.* **T12**, 34–42 (1986).
- N. Samantaray, "Quantum enhanced imaging and sensing with correlated light," Ph.D. thesis (Politecnico Di Torino, 2017).
- G. Agrawal, *Nonlinear Fiber Optics*, 5th ed. (Academic Press, 2012).
- R. H. Stolen, "Chapter 5: Nonlinear properties of optical fibers," in *Optical Fiber Telecommunications*, edited by S. E. Miller and A. G. Chynoweth (Academic Press, 1979), pp. 125–150.
- T. R. Hart, R. L. Aggarwal, and B. Lax, "Temperature dependence of Raman scattering in silicon," *Phys. Rev. B* **1**, 638–642 (1970).
- A. V. Masalov, A. Kuzhamuratov, and A. I. Lvovsky, "Noise spectra in balanced optical detectors based on transimpedance amplifiers," *Rev. Sci. Instrum.* **88**, 113109 (2017).
- K. Irie, A. E. McKinnon, K. Unsworth, and I. M. Woodhead, "A model for measurement of noise in CCD digital-video cameras," *Meas. Sci. Technol.* **19**, 045207 (2008).
- E. J. Allen, G. Ferranti, K. R. Rusimova, R. J. Francis-Jones, M. Azini, D. H. Mahler, T. C. Ralph, P. J. Mosley, and J. C. F. Matthews, "Passive, broadband, and low-frequency suppression of laser amplitude noise to the shot-noise limit using a hollow-core fiber," *Phys. Rev. Appl.* **12**, 044073 (2019).
- J. D. Mueller, N. Samantaray, and J. C. F. Matthews, "A practical model of twin-beam experiments for sub-shot-noise absorption measurements," data.bris (2020).